doi:10.2533/chimia.2015.41 Chimia 69 (2015) 41–51

Dye-sensitized Solar Cells: New Approaches with Organic Solid-state Hole Conductors

Nick Vlachopoulos[a], Jinbao Zhang[b], and Anders Hagfeldt[a]*

Abstract: Solid-state dye-sensitized solar cells (sDSCs) in which a solid organic charge-transfer medium, or hole conductor (HC), is interposed between a dye-coated mesoporous oxide electrode and a conductive counter electrode, have attracted considerable interest as viable alternatives to the more ubiquitous mediator-electrolyte DSC. Of particular importance to efficient operation are, in addition to the useful processes contributing to current generation (light harvesting, electron injection and current collection), the recombinative deleterious processes. The organic HCs are highly reactive toward electrons in the oxide or the conducting glass support, therefore necessitating the inclusion of a carefully prepared thin blocking oxide underlayer support as well as the molecular design of special dark current-suppressing dyes. Initially (mid-1990s) sDSCs with organic small molecular weight hole conductors have undergone systematic investigation. At the same time the first tests of sDSCs with conducting polymer hole conductors were published, with subsequent emphasis on the *in situ* generation of the HC inside the pores. For both types of devices a light-to-electricity conversion efficiency, in the 5-10% range for several dye-HC combinations, approaches that of the most efficient DSCs with non-volatile liquid electrolytes, thereby encouraging further efforts for obtaining stable, efficient and inexpensive sDSCs.

Keywords: Conducting polymer · Dye · Hole conductor · Mesoporous oxide·Solar cell

Introduction

Dye-sensitized solar cells (DSC*s*) have attracted considerable interest in the last quarter-century as candidates for electricity generation, not simply as alternatives to the traditional solid-state cells but also in special applications like building-integrated photovoltaics (smart windows) or indoor applications. The sensitization of semiconductor electrodes, including oxides (MO_x), has been the subject of several studies in the 1960s, 1970s and early 1980s; this earlier research has been reviewed by Memming.[1] In most of the earlier studies the photocurrents were very low, due to the fact that smooth electrodes were used for dye sensitization, resulting to weak dye adsorption at the electrode surface; a notable exception was the case of dyes adsorbed on porous ZnO, as reported by the Tsubomura group in a series of papers in the period 1976–1983;[2] this substrate is generated by sintering the oxide powder; in this case significantly enhanced photocurrents were recorded. The feasibility of efficient dye sensitization on porous high-surface area titanium oxide electrodes was first demonstrated in the 1980s by Michael Grätzel's laboratory in Lausanne, Switzerland[3,4] and the first patent for a DSC based on porous, high surface area TiO_2 electrodes was filed in February1987;[5] this series of studies has continued without interruption up to the present day. The potential of this technology was widely recognized after publication of the results of O'Regan and Grätzel[6] related to achievement of more than 7% of a power conversion efficiency (η) for a DSC with a Ru sensitizer attached on a colloidal (mesoscopic) TiO_2 electrode; the introduction of the latter type of substrate[7,8] has led to more efficient and easier to prepared DSCs.

General information about the properties of DSCs is available in a number of review papers.[9–14] The basic feature of this technology is the attachment of a dye at a high-surface oxide electrode by means of surface-attachment groups, in most cases carboxylate (COOH) groups; alternatively, cases of attachment *via* alternative groups like phosphonate ($–PO_2OH$) or boronate ($B(OH)_2$) have also been discussed in the DSC literature. Apart from TiO_2, the choice of dye substrate in the majority of DSC publications, other oxides, notably ZnO, SnO_2 and NiO (the latter p-type) have been extensively studied. As far as the supports of MO_x is concerned, in most cases transparent conducting oxide (TCO) layers on glass or plastic are used, usually fluorine-doped SnO_2 (FTO) or tin-doped In_2O_3 (ITO), and the cell is irradiated from the TCO electrode side (Fig. 1). This is the

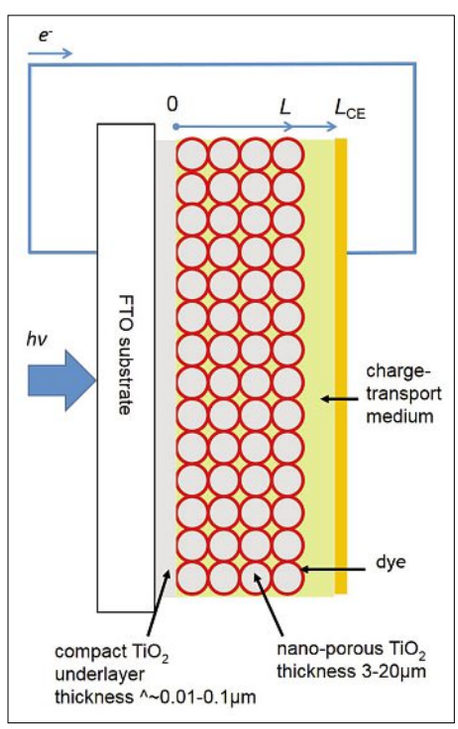

Fig. 1. Principles of dye solar cell operation.

*Correspondence: Prof. A. Hagfeldt[a]
E-mail: anders.hagfeldt@epfl.ch
[a]École Polytechnique Fédérale de Lausanne
Laboratory of Photomolecular Science
Institute of Chemical Sciences and Engineering
EPFL-FSB-ISIC-LSPM, Station 6
CH-1015 Lausanne, Switzerland
[b]Department of Chemistry-Ångström Laboratory
Uppsala University, Ångströmlaboratoriet
Lägerhyddsvägen 1, 75120 Uppsala, Sweden

case considered here. Of some interest is the use of opaque flexible metal substrates (iron, titanium) for MO_x; in this case illumination from a transparent counter electrode (CE) is necessary; otherwise the principles discussed below also apply.

The various steps involved in the DSC operation can be subdivided into the useful processes contributing to electricity generation and to the deleterious processes limiting cell performance. The useful processes (Fig. 2) are: (1) light absorption and excitation of an electron from the highest occupied (HOMO) to the lowest unoccupied (LUMO) orbital of the dye *D*; (2) electron transfer into the conduction band (CB) of MO_x and generation of the oxidized state of the dye *D* (D^+); (3) electron transfer from the semiconductor into the TCO/MO_x contact; (4) electron flow from photoelectrode to counter electrode with release of useful energy; (5) electron transfer from CE to the oxidized form of a redox mediator *Ox* in a liquid electrolyte or, equivalently, the oxidized (doped) entity in a solid-state hole conductor (HC) followed by diffusion of the generated electronated (reduced or undoped) species *Red* toward the photoelectrode; (6) reaction of *Red* with D^+ resulting to generation of *Ox* followed by *Ox* diffusing toward the CE. The deleterious processes (Fig. 3) are: (7) radiative (fluorescent) or nonradiative (heat generation) de-excitation of electrons in D^*; (8) recombination of CB electrons with *Ox*; (9) recombination of CB electrons with D^+; (10) recombination of electrons from TCO support with *Ox*; (11) recombination of electrons from TCO support with D^+. In order to suppress recombination reactions (10) and (11) a thin, compact oxide underlayer (blocking layer, buffer layer), of thickness of the order of 0.01–0.1 μm, is interposed between the TCO substrate and the mesoporous oxide layer. In the earlier version of the dye solar cell such an underlayer was not necessary due to the slow electrochemical kinetics of the triiodide mediator at a TCO layer without an electrocatalyst. However, in the case of several alternatives, more electroactive redox mediators (*e.g.* cobalt coordination complexes, organic heterocyclic redox mediators), and especially for organic hole conductors, such an underlayer is unavoidable, and the quality of it is often the determining factor for efficient operation.

Photon-to-Current Conversion

The incident photon-to-current conversion efficiency (IPCE) is given as the product of the light-harvesting efficiency of the surface-attached dye (LHE), the electron injection efficiency (φ_{inj}) from the excited dye into the conduction band, and the electron collection efficiency (φ_{inj}) at the MO_x/TCO interface.

$$IPCE = \mathrm{LHE} \cdot \varphi_{inj} \cdot \varphi_{coll} \qquad (1)$$

In the following each of the three terms will be discussed in some detail.

Light-harvesting Efficiency

The light harvesting efficiency (LHE) is expressed in terms of the photon fluxes of entering (I_{in}) and absorbed (I_{abs}) or, equivalently, exiting (I_{out}) light beam as

$$\mathrm{LHE} = \frac{I_{abs}}{I_{in}} = \frac{I_{in} - I_{out}}{I_{in}} \qquad (2)$$

At first any losses attributed to any factors other than absorption by the dye layer can be neglected. In that case LHE is expressed, for monochromatic light, by the Beer-Lambert law for surface-attached dye layers, by the equation in the integral form for a layer of thickness *L* (in cm) coated with a dye of uniform volume concentration *c* (in molcm^{-3})

$$I_{out} = I_{in} \exp(-N_A \sigma \Gamma) \qquad (3)$$

$$\mathrm{LHE} = 1 - \exp(-N_A \sigma \Gamma) \qquad (4)$$

where N_A is Avogadro's number, Γ is the surface concentration (mol/cm^2) based on the geometrical electrode surface, and σ is the molecular cross section for light absorption (wavelength-dependent, in cm^2 per molecule). Γ is related by the dye volume concentration *c* and the electrode thickness *L* for uniformly dyed electrodes as $\Gamma = cL$.

The usual form of the Lambert-Beer law, commonly used in solution but also applicable to dye-coated electrodes, is

$$\log \frac{I_{in}}{I_{in} - I_{abs}} = \varepsilon c L \qquad (5)$$

where ε is the molar extinction coefficient. σ and ε are related by

$$\sigma = \frac{ln10\varepsilon}{N_A} \qquad (6)$$

which is useful for light-harvesting calculations of adsorbed dyes if the same value of extinction coefficient is assumed for the dye dissolved in solution as in the surface-attached state.

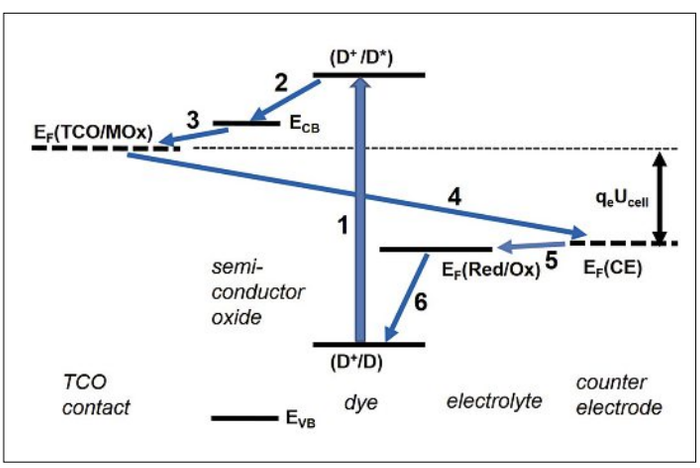

Fig. 2. Useful processes for dye solar cell efficient operation.

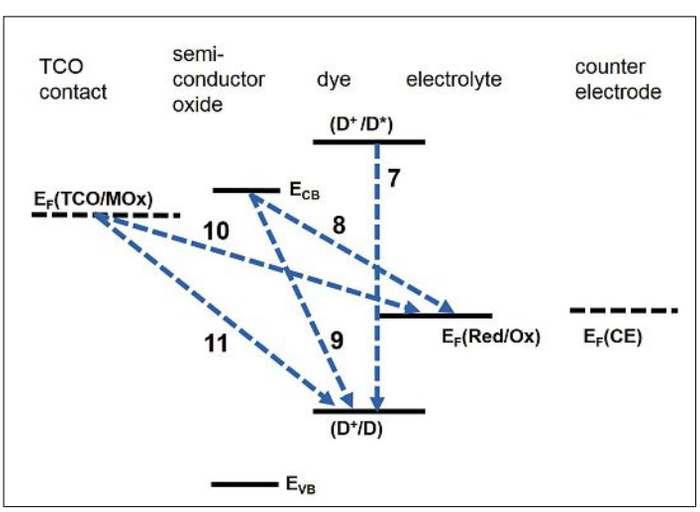

Fig. 3. Deleterious processes for dye solar cell efficient operation.

The surface concentration Γ_r of the adsorbed dye for full monolayer coverage can be calculated for a dye cross-section S_{dye} and a roughness factor (real/geometrical area) of r as

$$\Gamma_r\,/(\mathrm{molcm^{-2}}) = \frac{1.66\times10^{-10}\,r}{S_{dye}\,/\,\mathrm{nm^2molec^{-1}}} \quad (7)$$

LHE is expressed as a function of r, ε and S_{dye} by the following equation by considering that

$$\mathrm{LHE} = 1 - exp\left[-3.82\times10^{-7}\cdot r\cdot\frac{\varepsilon\,/\,\mathrm{Lmol^{-1}cm^{-1}}}{S_{dye}\,/\,\mathrm{nm^2}}\right] \quad (8)$$

Consider a smooth electrode (r = 1) of an inorganic coordination Ru dye with $\varepsilon_{max} = 10^4\mathrm{Lmol^{-1}cm^{-1}}$ at the maximum of the UV-VIS light absorption spectrum. Then if S_{dye} = 1 nm^2, LHE = 0.0038. Contrarily, for a porous colloidal mesoscopic oxide electrode, *e.g.* TiO_2 with r = 500 covered by the same dye, LHE = 0.85. The LHE values in the case of an organic coordination dye with higher absorbance, *e.g.* $\varepsilon_{max} = 5\times10^4\mathrm{Lmol^{-1}cm^{-1}}$, are 0.02 for r = 1 and close to unity for r = 500. In practice incident light losses due to absorption by the glass substrate, coloured components in the electrolyte or reflection at the glass substrate-air interface (for irradiation from the glass side) or both glass–air and photoelectrode–electrolyte (for irradiation from the electrolyte side) should be considered.

Electron Injection Efficiency

One absorbed photon impinging on the dye layer leads to the creation of an excited dye molecule D^*. By considering electron injection into the MO_x conduction band as the next step

$$D^* \xrightarrow{k_{inj}} D^+ + e \quad (9)$$

the electron injection efficiency (φ_{inj}) expresses effectiveness of the above process as compared to the excited state radiative or nonradiative deactivation

$$D^* \xrightarrow{k_{deact}} D \quad (10)$$

In terms of first-order kinetic constants

$$\varphi_{inj} = \frac{k_{inj}}{k_{inj} + k_{deact}} \quad (11)$$

Electron Collection Efficiency and Current

Electrons injected from D^* can either reach the TCO substrate, so that they contribute to the current flowing through the external circuit and toward the counter electrode; alternatively they can undergo deactivation (recombination) by reacting either (a) with the oxidized dye D^+ generated after electron injection from D^* or (b) with the oxidized form Ox of the redox mediator Red/Ox (or hole-conducting charge-transport system). We assume a simple one-electron redox system).

$$e_{\mathrm{MO_x}} + D^+ \rightarrow D \quad \text{with rate} \quad k_{rec\text{-}1}\cdot n\cdot C_{D^+} \quad (12)$$

$$e_{\mathrm{MO_x}} + Ox \rightarrow Red \quad \text{with rate} \quad k_{rec\text{-}2}\cdot n\cdot C_{Ox} \quad (13)$$

where n is the semiconductor electron concentration. The rate constants have units of molcm^{-2}s^{-1}. In treating mesoporous oxide electrodes it is customary to consider the interspersed oxide and electrolyte mixture as a medium and refer the concentrations of all species with respect to this medium.

In case of efficient regeneration of D from D^+ by reaction with Red according to step (c)

$$D^+ + Red \rightarrow D + Ox \quad (14)$$

the contribution of step (a) can be negligible. In this case only pathway (b) is effective for recombination. Step (a) has to be considered either in case of total absence of Red or of sluggish regeneration (c). In the following analysis only recombination step (b) will be considered.

The electron collection efficiency can be expressed in terms of the rates of electron collection and electron recombination as

$$\varphi_{coll} = \frac{R_{coll}}{R_{coll} + R_{rec\text{-}\mathrm{MOx}}} \quad (15)$$

where

$$R_{rec\text{-}\mathrm{MOx}} = \int_0^L k_{rec\text{-}2}\cdot n(x)\cdot C_{Ox}(x)\cdot\sigma_{\mathrm{MOx}}dx \quad (16)$$

R_{coll} and $R_{rec\text{-}\mathrm{MOx}}$, in units of molcm^{-2}s^{-1}, refer to one cm^2 of electrode cross-section. σ_{MOx} is the real area of the MO_x material per volume unit. The fact that the electron concentration and the concentration of the redox mediator are variable has been taken into account in the above equation. x is the position within the MO_x layer; x = 0 corresponds to the MO_x/TCO interface and x = L to the edge of the oxide layer facing the counter electrode. The rate $r_{rec\text{-}\mathrm{MOx}}$ of recombination per surface unit at position x is correspondingly

$$r_{rec\text{-}\mathrm{MOx}} = k_{rec\text{-}2}n(x)\,C_{Ox}(x) \quad (17)$$

R_{coll} can be expressed in terms of the electron diffusion flux injected into TCO

$$R_{coll} = D_n\left(\frac{dn(x)}{dx}\right)_{x=0} \quad (18)$$

where x = 0 corresponds to the position of the TCO/MO_x boundary.

In the case of the absence of dark current, *i.e.* of reduction of Ox by the electrons originating from the TCO material, R_{coll} is directly related to the current density J toward the external circuit; as

$$FR_{coll} = FD_n\left(\frac{dn(x)}{dx}\right)_{x=0} \quad (19)$$

Therefore

$$\varphi_{coll} = \frac{D_n\left(\frac{dn(x)}{dx}\right)_{x=0}}{D_n\left(\frac{dn}{dx}\right)_{x=0} + k_{rec\text{-}2}\cdot\int_0^L n(x)\cdot C_{Ox}(x)\cdot\sigma_{\mathrm{MOx}}\,dx} \quad (20)$$

If a dark (recombination) current from TCO is generated, then it should be equal to

$$j_{rec,\mathrm{TCO/MO_x}} = -F\cdot k_{rec,\mathrm{TCO/MO_x}}\cdot C_{Ox}(0)\cdot n(0) \quad (21)$$

The total current will be

$$j = FD_n\left(\frac{dn}{dx}\right)_{x=0} + j_{rec,\mathrm{TCO/MO_x}} \quad (22)$$

where $k_{rec,\mathrm{TCO/MOx}}$ is an electrochemical rate constant, depending on the Fermi level $E_{F(\mathrm{TOC/MOx})}$ of the TCO support. A typical expression has the form

$$k_{rec,\mathrm{TCO/MOx}} = k^{\bullet}_{rec,\mathrm{TCO/MOx}}\exp\left(\frac{\alpha_{\mathrm{TCO/MOx}}\;E_{F(\mathrm{TCO})}}{kT}\right) \quad (23)$$

with α being the transfer coefficient (usually $\alpha \approx 0.5$).

In the case of an oxide underlayer (UL) between TCO and MO_x the rate of electron transfer ($k_{rec,\mathrm{UL/MOx}}$) can, in principle, be described by a similar equation; however the value of $k^*_{rec,\mathrm{UL/MOx}}$, and, consequently, $k_{rec,\mathrm{UL/MOx}}$ will be substantially reduced.

If the electrode potential vs. the reference electrode is sufficiently positive, *i.e.* the difference $E_{CS} - E_{F(\mathrm{MOx})}$ between the conduction band at the electrode surface and the Fermi level in the MO_x bulk is sufficiently large, then $n(x)$ will be sufficiently low so that the second terms of the denominator of Eqn. (20) will be much smaller than the first term and $\varphi_{coll} \approx 1$. This is the condition which should be applied during IPCE measurements so that

$$IPCE = LHE\cdot\varphi_{inj} \quad (24)$$

The maximal (usually short-circuit) current density of the solar cell, indepen-

dent on the cell potential will be expressed in terms of the solar spectrum as

$$j_{max} = F\int_{\lambda_{(min)}}^{\lambda_{(max)}} \varphi_{inj} LHE(\lambda) I_{ph}(\lambda) d\lambda \quad (25)$$

$$I_{ph}(\lambda) = \frac{P(\lambda)\lambda}{hcN_A} \quad (26)$$

where $J_{ph}(\lambda)$ and $P(\lambda)$ are the photon flux and the power between $\lambda_{(min)}$ and $\lambda_{(max)}$, the limits of light absorption of the dye, per wavelength unit, F is the Faraday constant, h is the Planck constant, and c is the speed of light. Usually $P(\lambda)$ is obtained from solar energy distribution tables and $\varphi_{coll}\times$LHE(λ) is obtained by photocurrent spectroscopy measurements in the laboratory; it is common practice to compare calculated j_{max} to experimental j_{max} as determined by current-potential measurements in the laboratory.

Determination of the Current–Potential Characteristic Curve at the Photoelectrode: Keynote Concepts

The details of mathematical models for dye solar cells are beyond the scope of the present review. For a more complete analysis specialized publications of DSC modelling can be consulted.[15–18] In this respect only some points important for understanding the functioning of DSCs will be mentioned. Usually it is assumed that within the interdispersed dye-oxide-charge-transport medium (CTM) electrode layer the macroscopic electrical field is very low so that charged entities move by diffusion only. Therefore the conduction and valence band edges of the semiconductor will be flat; the (quasi-) Fermi level of electrons will fluctuate solely because of varying electron concentration. If $x = 0$ is the position of the TCO/MOx contact

$$E_{F(MO_x)}(x) = E_C + kT\ln\frac{n(x)}{N_C} \quad (27)$$

where E_C and N_C indicate the conduction band edge and N_C the effective density of energy states in the conduction band.

An additional feature of mesoscopic colloidal oxides used in DSCs is the low doping level; in conjunction to the large band-gap this indicates that there are practically no holes in the material under the conditions of normal DSC operation; therefore, electron-hole recombination is not under consideration and the only way for electrons to be depleted within the MO_x layer is by recombination with *Ox* (for sufficiently fast dye regeneration rate, as explained above). Consider a thin slab at position x within the layer of thickness dx. For any species C (n, *Ox*, *Red* or inert species S) the following equation is applicable for the rate of net generation ($R_{net\text{-}gen}$), *i.e.* generation minus disappearance (recombination)

$$D\frac{d^2C(x)}{dx^2} + R_{net-gen}(x) = 0 \quad (28)$$

where D is the diffusion coefficient; the diffusion coefficient in the CTM-MO_x interpenetrating layer ($D_{CTM\text{-}MOx}$) is different from that in a normal CTM medium. At first approximation the two coefficients are related to the porosity ε_p (fraction of free space) in the porous MO_x layer

$$D_{CTM-MO_x} = D_{CTM}\varepsilon_p \quad (29)$$

For electrons the rate of net generation is equal to the rate of light harvesting multiplied by the electron injection efficiency; for monochromatic light it is

$$R_{net-gen}^{electrons}(x) = \int_{\lambda_{min}}^{\lambda_{max}} \varphi_{inj}\,\alpha_\lambda\, I_{ph}(\lambda) \exp(-\alpha_\lambda x)\,d\lambda - k_{rec\text{-}2}\cdot n(x)\cdot C_{Ox}(x)\cdot\sigma_{MOx} \quad (30)$$

with $\alpha_\lambda = N_A\sigma_\lambda c_{dye}$ the light absorption coefficient. The first term of the above equation corresponds to electron generation according to the differential form of the Lambert-Beer Law. It is assumed that the beam enters at $x = 0$. The rate of recombination is defined by $k_{rec\text{-}2}\cdot C_{Ox}(x)\cdot n(x)$ as described above.

In case of very fast regeneration of the oxidized dye by reaction with *Red* the rate of this process is equal to the rate of electron injection.

For *Ox* the rate of dye generation is equal to the rate of electron injection on the basis of the assumption of very fast regeneration and the assumption of a very low and constant concentration of oxidized dye (steady-state principle); therefore the rates of net generation for *Ox* and *Red* are expressed as

$$R_{net-gen}^{Ox}(x) = \int_{\lambda_{min}}^{\lambda_{max}} \varphi_{coll}\alpha_\lambda\, I_{ph}(\lambda) \exp(-\alpha_\lambda x)d\lambda - k_{rec\text{-}2}\cdot n(x)\cdot C_{Ox}(x)\cdot\sigma_{MOx} \quad (31A)$$

$$R_{net-gen}^{Red}(x) = -\int_{\lambda_{min}}^{\lambda_{max}} \varphi_{coll}\alpha_\lambda\, I_{ph}(\lambda) \exp(-\alpha_\lambda x)d\lambda + k_{rec\text{-}2}\cdot n(x)\cdot C_{Ox}(x)\cdot\sigma_{MOx} \quad (31B)$$

In fact

$$R_{net-gen}^{electrons}(x) = R_{net-gen}^{Ox}(x) = -R_{net-gen}^{red}(x) \quad (32)$$

In the case of inert ions the rate of net generation is zero: therefore their concentration will be constant within the dye–electrolyte layer. Additionally, the electroneutrality condition should be considered: with a very low electric field the charge density in the electrolyte should be virtually zero, *i.e.* for electrons, *Red*, *Ox* and inert charged species S_i with charge z_i it should be

$$z_{Ox}(Ox) + z_{Red}(Red) - n + \sum_j z_j(S_j) = 0 \quad (33)$$

whence for a simple one-electron reaction $z_{Red} = z_{Ox} - 1$.

In addition to the electroneutrality the total amount of *Ox* and *Red* should be constant, defined by the amounts initially introduced upon preparation of the cell. The proportion *Red*/*Ox* will change during photoelectrochemical cell operation. When the DSC device is prepared in the dark the MO_x layer is virtually insulating; during operation of the photoelectrochemical cell it is populated by electrons. In order to maintain electroneutrality in the cell the amount of the oxidized form under light should increase over that in the dark. Therefore the initially added concentrations should be modified during cell operation. However, the mass balance for the mediator can be formulated as

$$\int_0^{L_{CE}} \{C_{Ox}(x) + C_{Red}(x)\}dx = \{C_{Ox}(in) + C_{Red}(in)\}L_{CE} \quad (34)$$

where C_{Ox}(in) and C_{Red}(in) are the concentrations initially added. L_{CE} is the total electrolyte thickness including the electrolyte-permeated oxide layer and the free electrolyte layer, as explained below (Fig. 1).

The above formalism is valid in case of both redox mediators dissolved into an inert electrolyte and solid-state HCs. In the case of the latter media charge transport takes place by electron hopping between either low-molecular weight molecules or monomeric units in a polymer chain. Diffusion of a hole is equivalent to the diffusion of an oxidized molecular entity, an organic molecule (*e.g.* spiro-OMeTAD, see in the following sections) or a monomeric unit in a conducting polymer chain (*e.g.* EDOT in a PEDOT conducting polymer), to the same direction. In that case the diffusion coefficients of *Ox* and *Red* are equal.

In addition to the boundary condition about the current at the MO_x/TCO boundary the conditions at the border of the MO_x layer ($x = L$) facing the counter electrode (CE) should be considered. In practice there is a layer of CTM separating the MOx electrode from the counter electrode ($L < x < L_{CE}$) with the counter electrode positioned at L_{CE}). At $x = L$ the electron flow in the semiconductor toward the counter electrode should be blocked, so that

$$\left(\frac{dn(x)}{dx}\right)_{x=L} = 0 \quad (35)$$

As regards diffusion from the MO_x-CTM layer into the free CTM layer the flux of species other than electrons should be the same; the diffusion coefficient of each species are different in the two layers

$$\left(D_{MO_x-CTM}\frac{dC_{MO_x-CTM}(x)}{dx}\right)_{x=L} = \left(D_{CTM}\frac{dC_{CTM}(x)}{dx}\right)_{x=L} \quad (36)$$

The modelling of diffusion and migration (field-assisted movement) in the free TCM layer can be undertaken by the well-known methodology of electrochemical engineering; for thin layers and sufficiently conductive CTM layer the migration effect can be neglected. At the counter electrode the reduction kinetics can be described by an equation analogous to that for the case at the TCO photoelectrode support, which for simple reactions can be written as

$$j_{CE} = F\left\{C_{Red}(L_{CE})k^{\bullet}_{CE-an}\exp\left(-\frac{(1-\alpha_{CE})E_{F(CE)}}{kT}\right) - C_{Ox}(L_{CE})k^{\bullet}_{CE-cath}\exp\left(\frac{\alpha_{CE}E_{F(CE)}}{kT}\right)\right\} \quad (37)$$

The currents at the photoelectrode and counter electrode are equal in magnitude and opposite in direction; under normal cell operation (with cell potential lower than the open-circuit value) under illumination it is

$$j_{TCO/MOx} = -j_{CE} = j_{CELL} \text{ and } j_{TCO/MOx} > 0 \quad (38)$$

The cell potential U_{cell} (in V) expressed in terms of Fermi levels, where Q^0 is the elementary charge of electricity, is

$$U_{CELL} = \frac{E_{F(TCO/MOx)} - E_{F(CE)}}{Q^0} - j_{CELL}R_{int} \quad (39)$$

where R_{int} is the ohmic resistance of the cell (including contributions from the resistance of the electrolyte and the electrode materials; the latter is particularly important for dye solar cells due to the high resistance of the TCO support of the photoelectrode and, eventually, the counter electrode.

The current–potential characteristic can be derived by the following procedure: $E_{F(TCO/MOx)}$ (or, equivalently, the electrode potential vs. a reference electrode) is specified as a boundary condition. Then concentrations $n(x)$, $C_{Ox}(x)$ and current $j_{TCO/MOx}$ are derived; at $x = L_{CE}$ by combining Eqns (27), (30) and (31), $E_{F(CE)}$ and U_{CELL} are evaluated. On the basis of incident light intensity P_{in} (Wcm^{-2}), cell current density j_{CELL} and cell potential U_{CELL}, the maximal energy conversion efficiency (η_{max}) and fill factor (*ff*), with j_{CELL} and U_{CELL} measured at the maximum cell power (P_{CELL}, in Wcm^{-2} units) point are expressed as

$$\eta_{max} = \frac{(P_{CELL})_{max}}{P_{IN}} = \frac{(j_{CELL}U_{CELL})_{max}}{P_{IN}} \quad (40)$$

$$ff = \frac{P_{CELL}}{P_{CELL(ID)}} = \frac{j_{CELL}U_{CELL}}{j_{CELL(SC)}U_{CELL(OC)}} \quad (41)$$

where $j_{CELL(SC)}$ and $U_{CELL(OC)}$ denote short-circuit current (highest cell current, photoelectrode and counter electrode at same potential) and open-circuit cell potential (highest cell potential, infinite resistance and therefore no current between photoelectrode and counter electrode) respectively; under ideal conditions, *i.e.* very fast kinetics at both electrodes and negligible cell resistance, a rectangular j_{CELL} vs. U_{CELL} characteristic should be derived, with

$$P_{CELL} = P_{CELL(ID)} = j_{CELL(SC)}U_{CELL(OC)} \quad (42)$$

In the following paragraphs the application of the aforementioned principles to organic HCs, with emphasis on conducting polymers, will be further elucidated.

Hole Transport in the Organic Medium

Three types of hole transport can be contemplated in the case of organic HCs: by polarons, by traps and electron hopping.[19,20] A polaron is an electron together with the positive charge induced by polarization of the surrounding medium. This type of transport is common for several conducting polymers. The transport by traps is analogous to that proposed for a mesoscopic oxide electrode; it takes place by successive trapping in a localized energy state and de-trapping by promotion into a continuous band lying energetically above the trap states. It occurs when the material is relatively rich in defects. Hole hopping involves a jump between two adjacent filled and empty lattice sites. In fact the exact mechanism of conduction in organic semiconductors is not well established, especially for low molar mass HCs, and distinguishing between the three aforementioned mechanisms is not always straightforward; for polymeric HCs the polaron model is commonly accepted. At low temperatures and at a low density of charge carriers electron hopping is favored; at more elevated temperatures and higher carrier density polaron formation can be expected. The density of carriers can be influenced by doping, as further explained in the sections dedicated to the particular HC materials; doping on the one hand increases the number of holes while, on the other hand, it contributes to a decrease of the hole mobility due to lattice distortion; at a low doping density (below 1%) the latter effect would predominate so that higher doping would be necessary to enhance the overall conductivity.

Three techniques can be applied for the measurement of the hole mobility (velocity per unit electric field): time of flight (TOF), dark-injection space-charge-limited current measurement (DI-SCL-C) and space-charge-limited current-voltage (SCL-CV) transient measurement.[21] In the TOF approach[22] the HC is placed between two electrodes, one of which is transparent or semi-transparent (*e.g.* transparent conducting oxide glass). A high hole concentration is created by a light pulse at the proximity of one of the electrodes. The drift of the pulse causes a continuous change of the field between the two electrodes and, therefore, to the charge density at their surface, so that a current is generated at the circuit between the two electrodes; an adequate bias potential is maintained between them. From the current vs. time transient a characteristic time of flight and subsequently, the mobility are derived. In the DI-SCL-C method a voltage pulse is applied in the dark and from the current transient the mobility is derived. In SCL-CV measurements the current is proportional to the square of applied voltage, and from the slope the hole mobility is obtained. The dependence of the mobility on the temperature can give an indication of the particular mechanism of hole transport. For polaron-based transport the decrease of mobility (μ) with temperature follows an Arrhenius-type dependence ($ln\mu \propto 1/T$). For hopping the behavior deviates from linearity; in several cases $ln\mu \propto 1/T^2$. These considerations can be further complicated by the fact that the mobility is often field-dependent; then the relation of μ vs. T would rather involve the mobility at low field strength E ($ln\mu(0)$ for $E \rightarrow 0$).

Introducing the Organic Solid into the Pores

The introduction of the HC into the pores of the mesoporous oxide is a prerequisite for efficient solar cell operation.[19] For low molar mass HCs, heating above the melting point is in principle possible. However, the required temperature should not be too high for the dye to decompose. The commonly used HC OMeTAD (also known as spiro-OMeTAD) has a melting

point around 250 °C, making this approach unsuitable for most dyes; this is a drawback of this otherwise efficient HC. The melting approach has been applied for an alternative HC, of melting point below 150 °C; however, the efficiency of the related DSC device is lower than that of OMeTAD-containing devices.[23] The most common approach for OMeTAD and other HCs is casting and evaporation of a liquid solution in a volatile solvent; usually spin-coating is effective for rapid solvent evaporation. The same approach is also applicable for the deposition of pre-formed, *i.e.* generated outside the TiO_2 layer, conducting polymer HCs.[24]

However, total filling of the pores of the oxide is not always achievable. Initially an amount of solution in excess of that required for filling the pores is added. During evaporation the concentration of HC in the capping layer (or overstanding layer, above the TiO_2 porous layer) is higher than that inside the pores so that a diffusion from the capping layer to the pores takes place; this concentration gradient will decrease with more slow spin-coating. At one point the capping solution is saturated; either precipitation of HC takes place or a gel is formed. At that point further diffusion into the pores stops so that the volume fraction of HC and additives in the saturated overstanding layer will determine the highest possible fraction of pore filling. The last stage of spin coating will totally eliminate the solvent so that an almost compact overlying HC later covers a partially filled oxide layer. Complete filling of the pores requires that the HC and the solvent are mutually soluble in all molar fractions, that the diffusion of HC is sufficiently fast at all concentrations, and that the spin coating process is sufficiently slow; the fulfillment of all these conditions for every efficient HC would not be self-evident. Electron microscopy can be used in some cases to evaluate the extent of pore filling. In some cases UV-VIS spectroscopic determination of the amount of HC in conjunction with evaluation of the mass of the capping layer can determine the extent of pore filling.[9] However, the essential point is that as long as the dye layer is completely covered by the solid HC and the latter forms a continuous phase inside the pores both dye regeneration and hole transport will take place; obviously the latter will be faster with higher pore filling. The establishment of a good contact between dye and HC can be evaluated by a relatively novel approach, photoinduced absorption spectroscopy (PIA), as elaborated for solid-state DSC studies in the authors' laboratory.[25] An electrode coated by dye and HC is irradiated by light of periodically varying intensity, and the intensity of the probe monochromatic light, of variable wavelength, is monitored by a detector coupled to a lock-in amplifier; in this respect the difference of absorbance between the illuminated and the dark condition is measured at the frequency of the light input, and the contributions of components not participating in the photoelectrochemical process is eliminated. In a typical experiment the spectrum obtained for a TiO_2-coated organic dye in contact with OMeTAD has been demonstrated to be that of OMeTAD only, without evidence of any amount of not-regenerated photooxidized dye in the porous TiO_2 layer; on the basis of this result virtually all dye is covered by the HC.

In the case of conducting polymers there is an additional approach of achieving efficient filling of the pores by generating *in situ* the polymer in the pores; the precursor is a low molar mass monomer or short oligomer, more readily oxidizable than the monomer, which can easily permeate the pores dissolved in an appropriate electrolyte. The polymer is generated *in situ* by photoelectrochemical polymerization (PEP), under constant potential (chronoamperometry) or current (chronopotentiometry). For chronoamperometry a three-electrode cell is required, with the photoelectrode potential controlled vs. a reference electrode. For chronopotentiometry a reference electrode is not required, but it is recommended, so that the process will be interrupted if the potential of the photoelectrode oversteps a certain threshold; in this way overoxidation of the polymer resulting to conversion to an insulating state is avoided. At the initial stage of the process the photooxidized dye is regenerated by hole injection into the precursor which can subsequently undergo dimerization by radical coupling; the reaction can continue with a coupling of the photooxidized precursor dimers with another photooxidized dimer or monomer, and so on. From the energetic point of view the longer a polymer chain, the easier its oxidation. The PEP method is analogous to the well-known electrochemical generation of conducting polymers at metal electrodes. However, the potential imposed to the photoelectrode is less positive to that required for polymerization at metals; electrons from the monomer or growing polymer are directly transferred to the ground state of the dye molecule, the Fermi level of which lies below that of the electrode, rather than to the electrode itself. This approach has been elaborated for the first time by the Yanagida group and further details will be presented in a following section.[26] *In situ* chemical polymerization of the monomer is also possible; in this case the procedure would be apparently simpler, without the requirement of electrochemical cell and instrumentation; however, chemical oxidants have to be introduced, and their excess amount as well as some by-products could have a deleterious effect to the quality of the HC film and result to parasitic reactions or lower hole mobility during cell operation.

Small Organic Molecule Hole Transport Materials

A quite detailed introduction to the above type of devices, covering the literature up to 2009, is provided by H. Snaith

Table 1. OF SDS devices based on spiro-TAD hole conductors: benchmark efficiencies achieved

No.	Year	Ref.	Dye code	Light int [%] AM1.5	Eff [%]	*Uop* [V]	*Isc* [mAcm^{-2}]	*ff*	Additives	CE
1	1998	[27]	Ru-N3	100	0.7	0.34	0.3	0.62	Sb,Li	Au
2	2001	[28]	Ru-N719	100	2.6	0.91	5.1	0.57	Sb,Li,TBP	Au
3	2002	[29]	Ru-N719	100	3.2	0.93	4.6	0.71	Sb,Li,TBP	Au
4	2005	[31]	Ru-Z907	100	4.0	0.75	8.3	0.64	Sb,Li,TBP	Au
5	2005	[39]	D102	100	4.1	0.87	7.7	0.62	Sb,Li,TBP	Au
6	2005	[32]	Ru-K51	10	4.6	0.78	0.8	0.75	Sb,Li,TBP	Au
7	2007	[33]	Ru-K68	100	5.1	0.86	11.0	0.68	Li,TBP	Ag
8	2010	[36]	C106	100	5.0	0.85	8.3	0.71	Li,TBP	Ag
9	2011	[41]	C220	100	6.1	0.88	9.7	0.71	Li, TBP	Ag
10	2011	[42]	Y123	100	7.2	0.99	9.5	0.76	Co, Li, TBP	Ag

Entry 3: Ag surface treatment, Ag added into dye bath. Entry 5: First efficient organic (metal-free) dye. Max. IPCE=60%. Entry 7: Dopant (*e.g.* Sb) eliminated for the first time, replacement of Au by Ag. Entry 8: Ru dye, 1st Certified 5% efficiency. Entry 9: Organic (metal-free) dye, highest certified efficiency. Entry 10: Organic (metal-free) dye, cobalt(II) complex FK102 added as dopant for the first time.

in the recent multi-authored book edited by Kalyanasundaram.[14,19] The first DSC operating with a solid HC medium was proposed by Bach *et al*.[27] in their keynote *Nature* paper in the context of a collaboration between Michael Grätzel's Lausanne group in the Swiss Federal Institute of Technology (EPFL), the Hoechst corporation of Germany (Donald Lupo), and the Max-Planck Institute of Polymer Science (MPI), Mainz, Germany (Josef Salbeck). An aromatic amine-type compound, 2,2′,7,7′-tetrakis(N,N-di-p-methoxyphenyl-amine) 9,9′-spirobifluorene (OMeTAD), was used as HC and an inorganic Ru dye (Ru-N3), $Ru(II)L_2(SCN)_2$, (L =4,4′-dicarboxy-2,2′-bipyridine), as sensitizer; at the time Ru-N3 (Table 1) was the most efficient sensitizer for liquid electrolyte, iodide-based, dye solar cells. OMeTAD is an amorphous solid at room temperature and the extensive branching structure would preclude crystallization, so that the hole mobility remains within reasonable limits. However, the melting point, or glass-transition temperature, is rather high, above 100 °C; in such an elevated temperature range OMeTAD would melt and penetrate the pores; a drawback is that several heat-sensitive dyes would start decomposing so that the preferred method of deposition would be spin-coating of a solution of the HC in chlorobenzene at ~0.2M concentration, close to the maximal solubility of OMeTAD. In this section OMeTAD will be the HC unless otherwise specified.

Between the porous TiO_2 layer and the transparent conducting oxide (TCO) support a thin compact TiO_2 underlayer was deposited by spray pyrolysis in order to block the recombination current from TCO. The counter electrode was a vacuum- evaporated gold layer. In the first device the solar-to-electrical energy conversion efficiency at the maximum power point (η) was 0.4%.

By addition of two additives, $N(PhBr)_3SbCl_6$ and salt LiTFSI (TFSI=$N(CF_3SO_2)_2$, η increased to 0.74%, corresponding to a maximum incident photon-to-electron efficiency ($IPCE_{max}$) of 33%. These values have to be contrasted with $IPCE_{max}$ exceeding 80% and η of 10% for iodide-based liquid solar cells of that time. $N(PhBr)_3SbCl_6$ acts as an oxidant; initially OMeTAD is added in the reduced state and the oxidized form $OMeTAD^{+\bullet}$ or possibly higher oxidation states; (OMeTAD contains four oxidizable amine groups) is needed for efficient hole conduction. The role of LiTFSI is more elaborate. Li^+, like H^+, is an acidic species determining the TiO_2 conduction band-edge (E_{CS}) at the electrode-HC interface. ion; With increasing amounts of Li^+ adsorbed on TiO_2 (E_{CS}) moves down (in the energy scale) and the driving force for electron transfer from dye excited state and semiconductor $E^*_{D/D+} - E_{CS}$) increases. Furthermore, it has been argued that in presence of Li^+ the rate of recombination between electrons injected into TiO_2 (e_{cb}) and $OMeTAD^{+\bullet}$ decreases due to the role of a Li^+ as a charge screen between e_{cb} and $OMeTAD^{+\bullet}$.

In an elaboration of the same device by the Lausanne group by Kruger *et al*.[28] the efficiency was further increased. The dye was a variety of Ru-N3, Ru-N719 (Table 1), with two of the four –COOH groups neutralized (–COO^--n-Bu4N^+); this ionization leads to an increase of the open-circuit voltage. Tert-butyl pyridine (TBP) was added; this basic compound contributes to a partial diminishment of the effect of the acidity of Li^+; a downward shift of (E^s_{cb}) has a positive effect on electron injection from dye excited state but can cause, at the same time, a decrease in the solar cell open-circuit voltage (U_{op}) (its theoretically maximal open-circuit value defined by the difference ($E_{CS} - E_F^{OMETAD/OMETAD+\bullet}$) between ($E^s_{cb}$) and the Fermi level ($E_F^{TAD/TAD+}$) of the HC). Moreover, TBP would play a similar role to that of Li^+ as a screen of the interaction between e_{cb} and $OMeTAD^{+\bullet}$. An additional advantage is related to the fact that the relative large TBP molecule upon adsorption on TiO_2 would contribute to the decrease of the reductive recombination current. Finally there is an advantage in the spin-coating process itself; the presence of the TBP increases the solubility of LITFSI in the aprotic solvent, and the increase of the solution polarity facilitates the penetration into the pores and ultimately leads to a better quality of the HC layer. In presence of $N(PhBr)_3SbCl_6$, LiTFSI and TBP, η reached 2.6% with U_{op} exceeding 900mV. A further study by the same researchers[29,30] demonstrated the possibility of further increasing U_{op}, and thereby η, to 3.2% , by the addition of Ag^+ ions into the dye deposition bath; this resulted in a more compact dye layer or eventually a bi-layer at the TiO_2 surface resulting to a decrease of recombination.

As alternative to the Ru-N3 dye, a Ru amphiphilic dye (Ru-Z907) with aliphatic chains attached to one of the ligands has been considered by Schmidt-Mende *et al*.[31] with the structure $Ru(SCN)_2LL'$, L = 4,4′-dicarboxy-2,2′-bipyridine and L′ = 4,4′-n-C_9H_{19}-2,2′-bipyridine. A solid-state DSC (sDSC) device with Z907 showed η = 4%, in the absence of Ag^+ treatment, higher than for the aforementioned studies[29] of cells with Ru-N3 dye (3.2%); the corresponding short-circuit currents were 8.3 $mAcm^{-2}$ (Ru-Z907) and 4.6 $mAcm^{-2}$ (Ru-N3). The increase of η can be attributed to the better packing of Ru-Z907 on TiO_2 to the long chains so that the light absorbance is higher than for Ru-N3 on an electrode despite the higher extinction coefficient of Ru-N3 in solution, resulting in higher photocurrents. The long chains will also contribute to the suppression of recombination and thereby to relatively high $U_{CELL(OC)}$. A further increase in η, to 4.6%, occurred with a similar sensitizer, RU-K51 (Table 1), containing ion-solvating polyether groups attached to L′.[32] The result of the Li^+ chelation by the dye is the establishment of an interfacial dipole causing a downward shift of ($E_F^{OMETAD/OMETAD+\bullet}$) with respect to ($E^s_{cb}$) so that the U_{op} and, consequently, η increase. Several amphiphilic dyes based on the Z907 ($Ru(SCN)_2LL'$) structure were elaborated by the Lausanne group in the following years based on the aforementioned structure. In some cases one of the –COOH groups of L is ionized with a Na^+ counterion.

The first cell which surpassed the 5% threshold, based on dye K68 (Table 1), is described by Snaith *et al.*[33] This dye contains ion-coordinating side ether groups; chelation of Li^+ by these groups has a positive effect to the suppression of dark current. In variance with previous device studies two modifications in cell composition were introduced in this article. Evaporated gold was replaced by silver; the advantage is the higher backward reflectivity of Ag for light impinging from the photoelectrode; therefore higher photocurrents are observed as indicated in a comparison of cells with Au, Ag and Au/Ag counter electrodes (Ag in the outer layer). Furthermore no oxidant (*e.g.* antimony salt) was added; in previous studies of Snaith and Grätzel[33] it was shown that addition of Sb at the usual doping level of 0.2% (fraction of the total molecules oxidized) does not increase the conductivity of the OMeTAD layer. Further studies by the Grätzel group involving high-efficiency were based on Ru dyes with the Z907 structure; in some cases sulphur-containing side groups (thiophene derivatives) were attached to the bipyridine ligand in L′.[34–38]

For all the aforementioned studies the optimal electrode thickness is 2–4 μm. This is due to the low hole mobility in conjunction with difficult pore filling for thick electrodes. This limitation can be overcome by using dyes with high extinction coefficient over a broad range of the solar spectrum. The Ru dyes mostly used in DSCs have a rather low maximal extinction coefficient ($\varepsilon_{max} = 10^4 M^{-1}cm^{-1}$) but a broad spectral distribution. Contrarily, several metal-free organic dyes of DSC interest have higher extinction coefficients (up to $\varepsilon_{max} = 5\times10^4 M^{-1}cm^{-1}$) but a rather restricted range of light adsorption. Therefore, because of the high ε_{max}, organic dyes have been the focus of intense investigations in the last 10 years; a synergy between organic chemists and device

specialists has been developed in view of developing strongly-absorbing novel dyes. The first report of an efficient sDSC based on an organic dye, of the indoline type (designated as indoline dye D102), supplied by the Mitsubishi Paper Mills Limited Company (Japan), was published by the Grätzel group; an 4.1% energy efficiency was attained.[39] The additives and Au counter electrode were the same as already mentioned. A systematic study of a series of metal-free charge-transfer dyes with a cyanoacrylic acid attachment group (electron acceptor) covalently linked to a triphenylamine moiety (electron donor) was performed in a collaborating effort of the Lausanne group, the present authors' Uppsala group, and their project collaborators, the group of Licheng Sun, in Stockholm.[40] Both the most efficient certified and the most efficient sDSC cells based on low molar mass HCs have been based on by organic sensitizers, C220 ($\eta = 6.1\%$) and Y123 ($\eta = 7.2\%$) respectively.[41,42] In the latter case the doping approach has been re-introduced, with a Co(III) coordination complex, FK102 (tris(2-(1H-pyrazol-1-yl)pyridine)cobalt(III)hexafluorophosphate, as dopant.

Up to this point OMeTAD was mentioned as HC, to the exclusion of other species. In fact this is the HC with which the highest η values were obtained. The best alternative HC, N,N,N′,N′-tetrakis(4-methoxyphenyl)benzidine (MeO-TPD) has been reported in a recent publication of the Uppsala group and their Stockholm collaborators in conjunction with the metal-free organic dye LEG4, structurally similar to the organic sensitizers described in the previous paragraph; with MeO-TPD $\eta = 4.9\%$ was obtained, vs. $\eta = 4.7\%$ for OMeTAD, with $U_{CELL(OC)} = 0.800$ V vs. 0.860 V and $j_{CELL(SC)} = 9.5$ mAcm^{-2} vs. 8.6 cm^{-2}, and $ff = 0.65$ vs. 0.62 respectively.[43] To achieve this result with MeO-TPD a light-soaking treatment, consisting of irradiating the cell under AM1.5 for 30 min, was essential; before this treatment $\eta = 1.1\%$. Contrarily, for the OMeTAD-based device the light soaking causes a slight degradation in efficiency. This treatment could be applied to other HCs in the future and lead to the establishment of efficient, inexpensive and stable HC-based cells with alternative to OMeTAD HCs.

Polymer HCs

Two main types of sDSCs based on polymers have been reported: these based on preformed polymers deposited by casting of a polymer solution in a solvent, with solvent evaporation usually by spin coating, and these in which the polymer was generated *in situ*, usually by photoelectrochemical polymerization (PEP). At first devices belonging to the first category will be discussed. Some of the oldest polymer-based DSCs, developed by the Sariciftci group in Linz (Austria) in the late 1990s–early 2000s, belong to the first type, with poly(3-octylthiophene) (P3OT) as HC and Ru-N719 dye.[44,45] No compact blocking underlayer suppressing the recombination current from the conducting glass was used; in spite of this the open-circuit cell potential ($U_{CELL(OC)}$) values as high as 0.7V were obtained, but the short-circuit photocurrent density ($j_{CELL(SC)}$) was below 1 mA/cm^2 and, consequently, η was below 0.2%. In subsequent years the use of pre-formed poly(3-hexylthiophene) (P3HT) as HC lead to more elevated η, as high as 3-4% in the best of cases, with organic dyes, *e.g.* CYC-B11[46] or D35.[47]

Among the earlier publications of *in situ* chemical or photochemical polymerization the following cases should be mentioned: Wang *et al.*[48] combined dye Ru-N3 with a polymeric HC, containing -COOH attachment groups, poly-carboxylated diacetylene; the polymer was generated into the pores of TiO_2 by *in situ* PEP; η was 0.8%; Saito *et al.* (Yanagida group, Japan)[26,49] chemically polymerized 3,4-ethylenedioxythiophene (EDOT), by Fe^{3+} as oxidant, to PEDOT in the pores of a TiO_2

Table 2. S-DSS devices based on conducting polymers: benchmark efficiencies achieved

No	Year	Ref.	Hole Cond.	Dye code	Irradiance [%] AM15	η [%]	*Uop* [V]	*Isc* [mAcm^{-2}]	ff	CE	El/lyte Added[a]
1	1998	[51]	Polypyrrole	N3	22	0.1	0.67	0.082	0.44		No
2	2002	[44]	P3OT	Ru-N719	80	0.2	0.65	0.45	0.44	Au	No
3	2003	[68]	MEHPPV	MEHPPV	100	0.5	0.75	0.64	0.54	Au	No
4	2004	[69]	P3TAA	P3TAA	100	1.1	0.42	4.1	0.63	Pt	No
5	2004	[52]	PEDOT[b]	Ru-N719	100	0.5	0.47	2.3	0.50	C	Yes
6	2004	[53]	PEDOT[b]	Ru-Z907	100	0.9	0.68	2.6	0.51	Au	Yes
7	2006	[55]	PEDOT[b]	Ru-HRS-1	10	2.6	0.78	4.5	0.74	Au	Yes
8	2008	[56]	PEDOT[b]	Ru-Z719	100	2.9	0.75	5.3	0.73	Au	Yes
9	2010	[60]	PEDOT[b]	D149	100	6.1	0.86	9.3	0.75	Pt	Yes
10	2011	[59]	PEDOT[b]	Ru-HRS-1	100	3.3	0.78	5.7	0.72	Ag	Yes
11	2012	[47]	P3HT	D35	100	3.2	0.88	6.8	0.53	Ag	No
12	2012	[46]	P3HT	CYC-B11	100	3.7	0.76	6.7	0.71	Au	No
13	2012	[61]	PEDOT[c]	D149	100	4.0	0.81	7.3	0.66	Au	Yes
14	2012	[62]	PEDOT[b]	D202	100	7.1	0.93	10.1	0.76	Au	Yes

[a] In several cases the polymer layer was impregnated for a few hours with a low-volatility electrolyte containing Li^+ (LiTFSI) and tert-bytylpyridine (TBP).
[b] Photoelectrochemical deposition of PEDOT from solution containing bis-EDOT e precursor.
[c] Photoelectrochemical deposition of PEDOT from solution containing a tris-EDOT derivative as precursor. Entry 1: Polypyrrole generated by photoelectrochemical polymerization of pyrrole. Entry 2: No compact underlayer and no low-volatility electrolyte added. Entry 3: MEHPPV as dye and hole conductor; PEDOT as charge-collection layer in contact with MEHPPV and counter electrode; no low-volatility electrolyte added. Entry 4: P3TAA as dye and hole conductor; more efficient cells obtained by impregnation with iodide-triiodide solution; no low-volatility electrolyte added. Entry 7: MoPEP deposition of PEDOT from bis-EDOT. Entry 8: PEP deposition of PEDOT from bis-EDOT. Entry 9: PEP deposition of PEDOT from bis-EDOT. Entry 11: Deposition of pre-formed P3HT; no low-volatility electrolyte added. Entry 12: Deposition of pre-formed P3HT; no low-volatility electrolyte added.

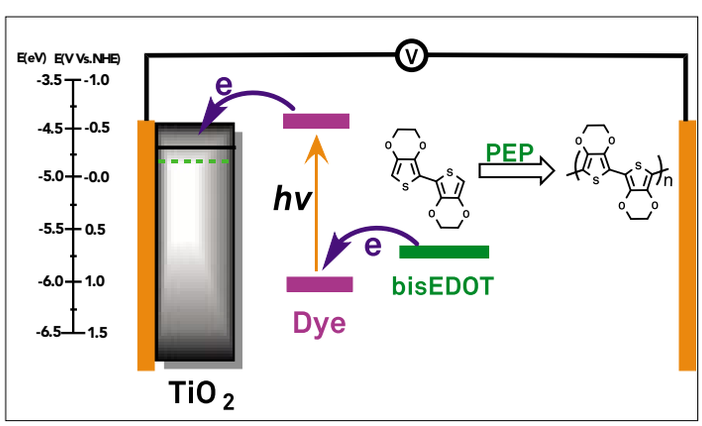

Fig. 4. Photoelectrochemical polymerization (PEP) for solid-state dye solar cells: principles of operation.

electrode coated with dye Ru-N719; η was only 0.1%. The same group presented the earliest examples of sDSCs with a conducting polymer as HC, polypyrrole, generated by PEP of pyrrole; with N3 as sensitizer η of *ca.* 0.1% was obtained.[50,51]

Later the focus was oriented toward investigation on PEDOT as HC in sDSCs generated by PEP (Figs. 4 and 5), with the Yanagida team playing a key role in the continuous improvement of performance. As precursor species in a nonaqueous solvent, typically acetonitrile, the dimer bis-EDOT and not EDOT was used due to the fact that bis-EDOT is more easily oxidized in PEP; the potential required for oxidation of EDOT is more positive than that corresponding to the ground state (HOMO) of the used dyes. In most of studies the dyes used were either Ru-N719, Ru-Z907 or a derivative of the latter with thiophene-containing side groups at the non-carboxylated bipyridine group, coded HRS-1.[26,52–59] The highest η was 3.1% with dye HRS-1 (Table 2).[59] In the same publication a comparison of various counter electrodes was presented; if the series (1) carbon paste (2) PEDOT (3) FTO-Ag paste is considered, for AM1.5 irradiation, I_{sc} slightly increases from (1) to (3); $U_{CELL(OC)}$ is almost identical for (1) and (2) but drastically increases from 0.46V to 0.78V from (2) to (3), resulting in the best overall η. This is attributed to the fact that some contact is established between counter electrode and photoelectrode; in this respect the contact Ag/TiO_2 would be more blocking than the contact with the other electrode materials.

A feature of all recent studies with photoelectropolymerized PEDOT is that a compact TiO_2 underlayer has been used in order to block the dark current; the demands for the quality of this underlayer are quite stringent due to the easy recombination reaction between the conductive polymer and any exposed sites of the conducting glass substrate. An additional feature is the addition of a liquid high boiling point electrolyte, typically propylene carbonate or ionic liquid, both containing a lithium salt and TBP base. After the photoelectropolymerization at the dye/oxide electrode the electrode is dipped into the electrolyte for some hours. The role of the above additives is in many aspects similar to that in the case of low molar mass HCs, as explained in the previous section; before cell assembly any excess electrolyte is removed from the electrode surface, but the electrolyte permeates the pores of the conducting polymer. Furthermore it has been claimed that the presence of liquid electrolyte at the oxide–polymer interface modifies its structure contributing to a decrease in the recombination current. However, such DSCs could be considered as not totally solid state devices. In this respect, as regards the final assembly of the solar cell the deposition of a metal counter electrode layer (*e.g.* Ag, Au) by evaporation is excluded due to the possible electrolyte degradation in the vacuum chamber. For that reason the counter electrode is either a Ag or C paste deposited without heat application or a conducting glass slide coated by a thin metal layer (usually Ag or Au), or eventually a conducting polymer layer, pressed against the photoelectrode.

Higher energy conversion efficiencies with PEDOT produced by PEP were obtained with metal-free, indoline-type organic dyes, D149,[60,61] and D205;[62] for the latter case η reached 7.1%, the highest for polymer-based DSCs reported up to the present. In one case[61] the polymer precursor was an EDOT trimer (tri-EDOT), the middle EDOT unit of which has an attached long-chain ether group so that the solubility is increases; the advantage is the ease of polymerization as compared to EDOT and bis-EDOT. In this respect η = 4.0% is obtained, higher than in previous studies with Ru-based dyes. All studies discussed above use electrolyte impregnation and a pressed counter electrode, as previously discussed.

The aforementioned system was further elaborated by the present authors and their collaborators in Uppsala University and in University Paris 7.[63–66] The more innovative point was the introduction of the principle of photoelectrochemical polymerization (PEP) in aqueous micellar solution. Apart from the environmentally friendly and inexpensive character of the process an additional advantage is the lower driving force for the polymerization process, as previously established by research related to electrochemical polymerization at conductive electrodes. In addition to the aqueous PEP of bisEDOT, PEP of monomer EDOT was achieved for the first time, exploiting the fact that polymerization of EDOT monomer requires considerable driving force in organic solution but much less in aqueous solution.[66] Another point is that the SDSC assembled in these studies did not include any non-volatile liquid electrode impregnation step. The best η, exceeding 5%, was obtained with organic charge-transfer sensitizers developed by the authors' Stockholm collaborators mentioned before, rather than with inorganic Ru dyes. In addition to PEDOT, efficient sDSCs (η exceeding 3%) were obtained for the first time with an alternative polymer, PEDOP, generated by nonaqueous PEP of the corresponding monomer EDOP.[67]

Up to this point the case of separate sensitizer and HC was mentioned. However, in further developments the possibility of a dye functioning simultaneously as light absorber and efficient HC would be of interest. A number of examples as regards DSC studies exist in the literature: Examples: a) the case of poly(2-methoxy, 5-(2′-ethyl-hexoxy)-1,4-phenylenevinylene) (MEHPPV) with η = 0.49% in the configuration ITO/TiO_2/TiO_2MEHPPV/PEDOT/Au, with two HCs, in series;[68] b) poly(3-thiophene acetic acid) (PTAA) with η = 1.1.% ($j_{CELL(SC)}$ = 4.1 mAcm^{-2} and $U_{CELL(OC)}$ = 0.42 V).[69]

The latter case was a part of an investigation of the possibility of combining a conducting polymer with an iodide/triiodide (I^-/I_3^-) redox mediator; conducting polymers, being ionic conductors as well, are of interest as solid supports for redox electrolytes, playing a similar role to that organic media like polyethylene oxide or polyacrylonitrile. Such cases are beyond the scope of the present review. One intermediate case is that of dual mediators. Mediator R_1/O_1 interacts with the dye, mediator Red_2/Ox_2 transports charge and interacts with the counter electrode according to the following scheme:

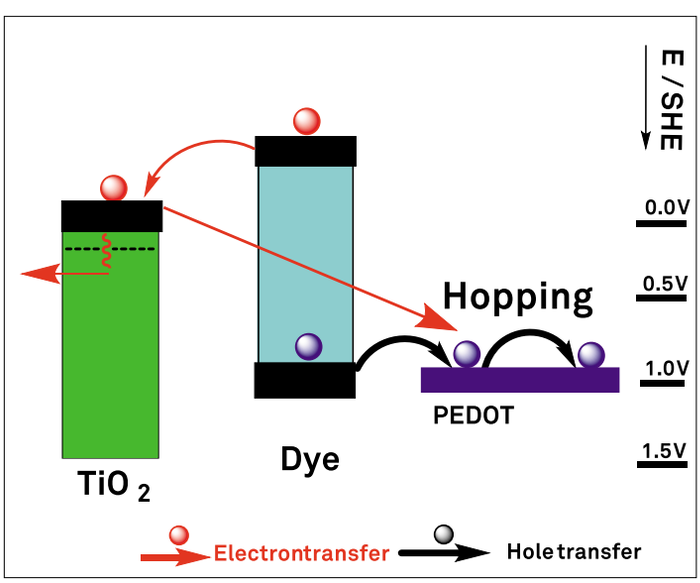

Fig. 5. Solid-state dye solar cell based on a conducting polymer: energy diagram.

$$D \xrightarrow{h\nu} D^* \rightarrow D^+ + e^-(\text{cb})$$
$$D^+ + Red_1 \rightarrow D + Ox_1$$
$$Ox_1 + Red_2 \rightarrow Ox_2 + Red_1$$
$$Ox_2(\text{PHE}) \rightarrow \text{Ox}_2(\text{CE})$$
$$Ox_2(\text{CE}) + e^-(\text{CE}) \Rightarrow Red_2(\text{CE})$$

For example, an often discussed case of iodine-free solid-state cells consists of an PEDOT layer impregnated with an ionic liquid containing I^- but not I_3^- (Ox_1); in this way the disadvantages due to I_3^- present in a substantial amount are largely avoided (substantial light absorption, volatility). The photooxidized dye transfers a hole to I^- generating I_3^-. In turn, I_3^- injects a hole to PEDOT (Red_2). Subsequently, $PEDOT^+$ (Ox_2) is transported toward and reduced at the counter electrode to PEDOT (Red_2). Hole transport between photoelectrode and counter electrode is assured by PEDOT/$PEDOT^+$ (Red_2/Ox_2). Strictly speaking this case lies also beyond the context of the present review. It is worth mentioning that such liquid–solid cells can achieve higher efficiencies than DSCs based solely on conducting polymers; *i.e.* 6.9% for a cell with Ru-N719 sensitizer, iodide-containing ionic liquid, and PEDOT (without triiodide) generated into the pores by chemical polymerization.[70,71] The same dual-mediator scheme applies for sDSC with two HCs. An example is the application of tris(p-anisyl)amine (TPAA) as regenerator (Ox_1) and P3HT as charge transporter (Ox_2) interacting with the counterelectrode; with sensitizer Ru-K77 it is $\eta = 0.2\%$.[72]

Table 3. Abbreviations for compounds mentioned in the text

Bis-EDOT	2,3-dihydro-5-(2,3-dihydrothieno[3,4-b][1,4]dioxin-5-yl)thieno[3,4-b][1,4]dioxine
C106	RuLL'(NCS)$_2$ (L=2,2'-bipyridyl-4,4'-dicarboxylic acid; L' = 4,4'-bis(5-(hexylthio)thiophen-2-yl)-2,2'-bipyridine))
C220	2-cyano-3-{6-{4-[N,N-bis(4-hexyloxyphenyl)amino]phenyl}-4,4-didodecyl-4Hcyclopenta[2,1-b:3,4-b´]dithiophene-2-yl}acrylic acid
CYC-B11	CYC-B11 (TBA(Ru[(4-carboxylic acid-4'-carboxylate-2,2'-bipyridine) {(4,4'-bis(5-(hexylthio)-2,2'-bithien-5'-yl)-2,2'- =-bipyridine) (NCS)2])}
EDOP	3,4-ethylenedioxypyrrole
EDOT	3,4-ethylenedioxythiophene
D35	(E)-3-(5-(4-(bis(20,40-dibutoxybiphenyl-4-yl)amino)phenyl)thiophen-2-yl)-2-cyanoacrylic acid
D102	(5-{4-[4-(2,2-diphenylvinyl)phenyl]-1,2,3,3a,4,8b-hexahydro-cyclopenta[b]indol-7-ylmethylene}-4-oxo-2-thioxo-thiazolidin-3-yl) acetic acid (indoline dye)
D149	5-[[4-[4-(2,2-diphenylethenyl)phenyl]-1,2,3-3a,4,8b-hexahydrocyclopent[b]indol-7-yl]methylene]-2-(3-ethyl-4-oxo-2-thioxo-5-thiazolidinylidene)-4-oxo-3-thiazolidineacetic acid
D205	5-[[4-[4-(2,2-diphenylethenyl)phenyl]-1,2,3,3a,4,8b-hexahydrocyclopent[b]indol-7-yl]methylene]-2-(3-octyl-4-oxo-2-thioxo-5-thiazolidinylidene)-4-oxo-3-thiazolidineacetic acid (indoline dye)
HRS-1	cis-Ru(4,4'-di(hexylthienylvinyl))(4,4'-dicarboxy-2,29-bipyridyl) (NCS)2 [dhtbpy = 4,4'-di(hexylthienylvinyl)-2,29-bipyridyl; dcbpy = 4,4'-dicarboxy-2,29-bipyridyl]
LEG4	(E)-3-(6-(4-(Bis(2',4'-dibutoxy-[1,1'-biphenyl]-4-yl)amino)phenyl)-4,4-dihexyl-4H-cyclopenta[2,1-b:3,4-b´]dithiophen-2-yl)-2-cyanoacrylic acid
P3HT	poly-(3-hexyl)thiophene
PC61BM	[6,6]-phenyl-C61-butyric acid methyl ester
PDI	N,N'-dialkyl perylenediimide
PEDOT	poly(3,4-ethylenedioxythiophene)
PEDOP	poly(3,4-ethylenedioxypyrrole)
Ru-K51	NaRu(4-carboxylic acid-4'-carboxylate)(4,4'- bis[(triethylene glycol methylether) methylether]-2,2'-bipyridine)(NCS)2
Ru-K68	NaRu(4-carboxylic acid-4'-carboxylate)(4,4´-bis[(triethyleneglycolmethylether) heptylether]-2,2'-bipyridine)(NCS)2
Ru-N3	cis-bis(isothiocyanato)bis(2,2'-bipyridyl-4,4'-dicarboxylato)-ruthenium(II)
Ru-N719	cis-diisothiocyanato-bis(2,2'-bipyridyl-4,4'-dicarboxylato) ruthenium(II) bis(tetrabutylammonium)
Ru-Z907	cis-disothiocyanato-(2,2'-bipyridyl-4,4'-dicarboxylic acid)-(2,2'-bipyridyl-4,4'-dinonyl) ruthenium(II)
TPD	N,N'-bis(3-methylphenyl)-N,N'-diphenylbenzidine
Y123	3-{6-{4-[bis(2,4-dihexyloxybiphenyl-4-yl)amino-]phenyl}-4,4-dihexyl-cyclopenta-[2,1-b:3,4-b2]dithiphene-2-yl}-2-cyanoacrylic acid

Summary and Outlook

Solid-state dye-sensitized solar cells have been extensively developed in the last twenty years, with the main motivation being the avoidance of a liquid charge-transport medium resulting to easier processability as well as the expectation of better stability. At first, low molecular weight hole conductors were considered, with considerable feedback and motivation from organic electronics-related developments; at a later stage, electronically conducting polymers have attracted considerable interest, in particularly those that can be deposited by photoelectrochemical polymerization, with the advantage of 'building up' the charge-transport solid medium into the pores of the mesoporous oxide layer. The energy conversion efficiencies achieved up to now, below 10%, are almost comparable to these of dye solar cells with redox mediators in non-volatile liquid electrolytes. The considerable versatility affordable by molecular design is expected to contribute to further optimization of these systems. Moreover, in the last five years several types of organic hole conductors investigated in solid-state dye solar cells have been successfully applied in solar cells with a perovskite layer as light absorber, with efficiencies up to 20%. Whether ultimately dyes or perovskites prevail, as not only efficient but also stable and inexpensive sensitizers, is difficult to predict; however, developments on dye solar cells with organic hole conductors will doubtless benefit the alternative application field as well.

Received: January 23, 2015

[1] R. Memming, *Prog. Surf. Sci.* **1984**, *17*, 7.
[2] M. Matsumura, S. Matsudaira, H. Tsubomura, M. Takata, H. Yanagida, *Ind. Eng. Chem. Prod. Res. Dev.* **1980**, *19*, 415.
[3] J. Desilvestro, M. Gratzel, L. Kavan, J. Augustynski, *J. Am. Chem. Soc.* **1985**, *105*, 2988.
[4] N. Vlachopoulos, P. Liska, J. Augustynski, M. Grätzel, *J. Am. Chem. Soc.* **1988**, *110*, 1216.

[5] M. Grätzel, P. Liska, United States patent No. 4927721, **1990**.
[6] B. O'Regan, M. Grätzel, *Nature* **1991**, *353*, 737.
[7] T. Gerfin, M. Grätzel, L. Walder, *Prog. Inorg. Chem.* **1997**, *44*, 345.
[8] C. J. Barbé, F. Arendse, P. Comte, M. Jirousek, F. Lenzmann, V. Shklover, M. Grätzel, *J. Am. Ceram. Soc.* **1997**, *80*, 3157.
[9] M. Grätzel, *Renew. Energy* **1994**, *5*, 118.
[10] A. Hagfeld, M. Grätzel, *Chem. Rev.* **1995**, *95*, 49.
[11] A. Hagfeldt, M. Grätzel, *Acc. Chem. Res.* **2000**, *33*, 269.
[12] M. Grätzel, *Nature* **2001**, *414*, 338.
[13] A. Hagfeldt, G. Boschloo, L. Sun, L. Kloo, H. Pettersson, *Chem. Rev.* **2010**, *110*, 6595.
[14] 'Dye-Sensitized Solar Cells', Ed. K. Kalyanasundaram, EPFL Press, Lausanne, Switzerland, **2010**.
[15] S. Sodergren, A. Hagfeldt, J. Olsson, S.E. Lindquist, *J. Phys. Chem.* **1994**, *98*, 5552.
[16] N. Papageorgiou, P. Liska, A. Kay, M. Grätzel, *J. Electrochem. Soc.* **1999**, *146*, 898.
[17] R. Stangl, J. Ferber, J. Luther, *Sol. Energy Mater. Sol. Cells* **1998**, *54*, 255.
[18] J. Ferber, J. Luther, *J. Phys. Chem. B* **2001**, *105*, 4895.
[19] H. J. Snaith, 'Solid-state dye sensitized solar cells', in 'Dye-Sensitized Solar Cells', EPFL Press, Lausanne, Switzerland, **2010**, pp. 163–206.
[20] H. Bässler, A. Köhler, *Top. Curr. Chem.* **2012**, *312*, 1.
[21] D. Poplavskyy, J. Nelson, *J. Appl. Phys.* **2003**, *93*, 341.
[22] W. E. Spear, *J. Non. Cryst. Solids* **1969**, *1*, 197.
[23] K. Fredin, E. M. J. Johansson, M. Hahlin, R. Schölin, S. Plogmaker, E. Gabrielsson, L. Sun, H. Rensmo, *Synth. Met.* **2011**, *161*, 2280.
[24] A. Abrusci, I.-K. Ding, M. Al-Hashimi, T. Segal-Peretz, M. D. McGehee, M. Heeney, G. L. Frey, H. J. Snaith, *Energy Environ. Sci*. **2011**, *4*, 3051.
25] U. B. Cappel, E. a. Gibson, A. Hagfeldt, G. Boschloo, *J. Phys. Chem. C* **2009**, *113*, 6275.
[26] Y. Saito, T. Azechi, T. Kitamura, Y. Hasegawa, Y. Wada, S. Yanagida, *Coord. Chem. Rev.* **2004**, *248*, 1469.
[27] U. Bach, D. Lupo, P. Comte, J. E. Moser, F. Weissörtel, J. Salbeck, H. Spreitzer, M. Grätzel, *Nature* **1998**, *395*, 583.
[28] J. Krüger, R. Plass, L. Cevey, M. Piccirelli, M. Grätzel, U. Bach, *Appl. Phys. Lett.* **2001**, *79*, 2085.
[29] J. Krüger, R. Plass, M. Grätzel, H.-J. Matthieu, *Appl. Phys. Lett.* **2002**, *81*, 367.
[30] J. Krüger, R. Plass, H. J. Matthieu, M. Grätzel, *Proc. SPIE* **2003**, *4801*, 56.
[31] L. Schmidt-Mende, S. M. Zakeeruddin, M. Grätzel, *Appl. Phys. Lett.* **2008**, *86*, 013504.
[32] H. J. Snaith, S. M. Zakeeruddin, L. Schmidt-Mende, C. Klein, M. Grätzel, *Angew. Chem. Int. Ed. Engl*. **2005**, *44*, 6413.
[33] H. J. Snaith, A. J. Moule, K. Meerholz, R. H. Friend, M. Gràtzel, *Nanoletters* **2007**, *7*, 3372.
[34] M. Wang, P. Chen, R. Humphry-Baker, S. M. Zakeeruddin, M. Grätzel, *Chemphyschem.* **2009**, *10*, 290.
[35] M. Wang, C. Grätzel, S.-J. Moon, R. Humphry-Baker, N. Rossier-Iten, S. M. Zakeeruddin, M. Grätzel, *Adv. Funct. Mater*. **2009**, *19*, 2163.
[36] M. Wang, J. Liu, N.-L. Cevey-Ha, S.-J. Moon, P. Liska, R. Humphry-Baker, J. E. Moser, C. Grätzel, P. Wang, S. M. Zakeeruddin, M. Grätzel, *Nano Today* **2010**, *5*, 169.
[37] M. Wang, S.-J. Moon, M. Xu, K. Chittibabu, P. Wang, N.-L. Cevey-Ha, R. Humphry-Baker, S. M. Zakeeruddin, M. Grätzel, *Small* **2010**, *6*, 319.
[38] M. Wang, S.-J. Moon, D. Zhou, F. Le Formal, N.-L. Cevey-Ha, R. Humphry-Baker, C. Grätzel, P. Wang, S. M. Zakeeruddin, M. Grätzel, *Adv. Funct. Mater.* **2010**, *20*, 1821.
[39] L. Schmidt-Mende, U. Bach, R. Humphry-Baker, T. Horiuchi, H. Miura, S. Ito, S. Uchida, M. Grätzel, *Adv. Mater.* **2005**, *17*, 813.
[40] S.-J. Moon, J.-H. Yum, R. Humphry-Baker, K. M. Karlsson, D. P. Hagberg, T. Marinado, A. Hagfeldt, L. Sun, M. Grätzel, M. K. Nazeeruddin, *J. Phys. Chem. C* **2009**, *113*, 16816.
[41] N. Cai, S.-J. Moon, L. Cevey-Ha, T. Moehl, R. Humphry-Baker, P. Wang, S. M. Zakeeruddin, M. Grätzel, *Nano Lett.* **2011**, *11*, 1452.
[42] J. Burschka, A. Dualeh, F. Kessler, E. Baranoff, N.-L. Cevey-Ha, C. Yi, M. K. Nazeeruddin, M. Grätzel, *J. Am. Chem. Soc.* **2011**, *133*, 18042.
[43] L. Yang, B. Xu, D. Bi, H. Tian, G. Boschloo, L. Sun, A. Hagfeldt, E. M. J. Johansson, *J. Am. Chem. Soc.* **2013**, *135*, 7378.
[44] D. Gebeyehu, C. J. Brabec, N. S. Sariciftci, D. Vangeneugden, R. Kiebooms, *Synth. Met.* **2002**, *125*, 279.
[45] D. Gebeyehu, C. J. Brabec, N. S. Sariciftci, *Thin Solid Films* **2002**, *404*, 271.
[46] W.-C. Chen, C.-Y. Chen, C.-G. Wu, K.-C. Ho, L. Wang, *J. Power Sources* **2012**, *214*, 113.
[47] L. Yang, U. B. Cappel, E. L. Unger, M. Karlsson, K. M. Karlsson, E. Gabrielsson, L. C. Sun, G. Boschloo, A. Hagfeldt, E. M. J. Jahansson, *J. Phys. Chem. C* **2012**, *116*, 18070.
[48] Y. Wang, K. Yang, S. Kim, R. Nagarajan, L. A. Samuelson, *Chem. Mater.* **2006**, *18*, 4215.
[49] Y. Saito, T. Kitamura, Y. Wada, S. Yanagida, *Synth. Met.* **2002**, *131*, 185.
[50] K. Murakoshi, R. Kogure, Y. Wada, S. Yanagida, *Chem. Lett.* **1997**, 471.
[51] K. Murakoshi, R. Kogure, Y. Wada, S. Yanagida, *Sol. Energy Mater. Sol. Cells* **1998**, *55*, 113.
[52] Y. Saito, N. Fukuri, R. Senadeera, T. Kitamura, Y. Wada, S. Yanagida, *Electrochem. Commun.* **2004**, *6*, 71.
[53] N. Fukuri, Y. Saito, W. Kubo, G. K. R. Senadeera, T. Kitamura, Y. Wada, S. Yanagida, *J. Electrochem. Soc.* **2004**, *151,* A1745.
[54] N. Fukuri, N. Masaki, T. Kitamura, Y. Wada, S. Yanagida, *J. Phys. Chem. B* **2006**, *110*, 25251.
[55] A. J. Mozer, Y. Wada, K.-J. Jiang, N. Masaki, S. Yanagida, S. N. Mori, *Appl. Phys. Lett.* **2006**, *89*, 043509.
[56] A. J. Mozer, D. K. Panda, S. Gambhir, T. C. Romeo, B. Winther-Jensen, G. G. Wallace, *Langmuir* **2010**, *26*, 1452.
[57] J. Xia, N. Masaki, M. Lira-Cantu, Y. Kim, K. Jiang, S. Yanagida, *J. Phys. Chem. C* **2008**, *112*, 11569.
[58] J. Xia, N. Masaki, M. Lira-Cantu, Y. Kim, K. Jiang, S. Yanagida, *J. Am. Chem. Soc.* **2008**, *130*, 1258.
[59] K. Manseki, W. Jarernboon, Y. Youhai, K.-J. Jiang, K. Suzuki, N. Masaki, Y. Kim, J. Xia, S. Yanagida, *Chem. Commun.* **2011**, *47*, 3120.
[60] X. Liu, W. Zhang, S. Uchida, L. Cai, B. Liu, S. Ramakrishna, *Adv. Mater.* **2010**, *22*, E150.
[61] L. Cai, X. Liu, L. Wang, B. Liu, *Polym. Bull.* **2011**, *68*, 1857.
[62] X. Liu, Y. Cheng, L. Wang, L. Cai, B. Liu, *Phys. Chem. Chem. Phys.* **2012**, *14*, 7098.
[63] L. Yang, J. Zhang, Y. Shen, B.-W. Park, D. Bi, L. Häggman, E. M. J. Johansson, G. Boschloo, A. Hagfeldt, A. Snedden, L. Kloo, A. Jarboui, A. Chams, C. Perruchot, M. Jouini, N. Vlachopoulos, *J. Phys. Chem. Lett.* **2013**, *4*, 4026.
[64] J. Zhang, L. Yang, Y. Shen, B.-W. Park, Y. Hao, E. M. J. Johansson, G. Boschloo, L. Kloo, E. Gabrielsson, L. Sun, A. Jarboui, C. Perruchot, M. Jouini, N. Vlachopoulos, A. Hagfeldt, *J. Phys. Chem. C* **2014**, *118*, 16591.
[65] B. Park, L. Yang, E. M. J. Johansson, N. Vlachopoulos, A. Chams, C. Perruchot, M. Jouini, G. Boschloo, A. Hagfeldt, *J. Phys. Chem. C* **2013**, *117*, 22484.
[66] J. Zhang, A. Jarboui, N. Vlachopoulos, M. Jouini, G. Boschloo, A. Hagfeldt, *Electrochim. Acta* **2015**, in press.
[67] J. Zhang, L. Häggman, M. Jouini, A. Jarboui, G. Boschloo, N. Vlachopoulos, A. Hagfeldt, *Chemphyschem.* **2014**, *15*, 1043.
[68] M. Y. Song, J. K. Kim, K.-J. Kim, D. Y. Kim, *Synth. Met.* **2003**, *137*, 1387.
[69] S. Yanagida, G. K. Senadeera, K. Nakamura, T. Kitamura, Y. Wada, *J. Photochem. Photobiol. A Chem.* **2004**, *166*, 75.
[70] J. Kim, J. K. Koh, B. Kim, S. H. Ahn, H. Ahn, D. Y. Ryu, J. H. Kim, E. Kim, *Adv. Funct. Mater.* **2011**, *21*, 4633.
[71] B. Kim, J. K. Koh, J. Kim, W. S. Chi, J. H. Kim, E. Kim, *ChemSusChem.* **2012**, *5*, 2173.
[72] E. M. J. Johansson, L. Yang, E. Gabrielsson, P. W. Lohse, G. Boschloo, L. Sun, A. Hagfeldt, *J. Phys. Chem. C* **2012**, *116*, 18070.